THE JOURNAL OF PHYSICAL CHEMISTRY B

Article

pubs.acs.org/JPCB

Glassy Behavior of Denatured DNA Films Studied by Differential Scanning Calorimetry

Jessica Valle-Orero,*[,†,‡] Jean-Luc Garden,[§] Jacques Richard,[§] Andrew Wildes,[†] and Michel Peyrard*[,‡]

[†]Institut Laue Langevin, BP 156, 6, rue Jules Horowitz 38042 Grenoble Cedex 9, France

[‡]Laboratoire de Physique, Ecole Normale Supérieure de Lyon, 46 allée d'Italie, 69364 Lyon Cedex 07, France

[§]Institut Néel, CNRS - Université Joseph Fourier, 25 rue des Martyrs, BP 166, 38042 Grenoble Cedex 9, France

ABSTRACT: We use differential scanning calorimetry (DSC) to study the properties of DNA films, made of oriented fibers, heated above the thermal denaturation temperature of the double helical form. The films show glassy properties that we investigate in two series of experiments, a slow cooling at different rates followed by a DSC scan upon heating and aging at a temperature below the glass transition. Introducing the fictive temperature to characterize the glass allows us to derive quantitative information on the relaxations of the DNA films, in particular to evaluate their enthalpy barrier. A comparison with similar aging studies on PVAc highlights some specificities of the DNA samples.

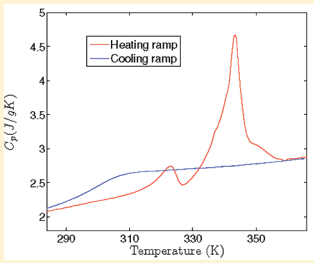

■ INTRODUCTION

The famous double helical structure of DNA, proposed by Watson and Crick,[1] was inferred from an X-ray image obtained with a DNA fiber. The fiber form of DNA, which can also be turned into a film of such fibers, is very important as it provides a unique way to get samples in which long DNA molecules are oriented. This allows for instance structural studies of genomic DNA.[2,3] Moreover the fiber and film forms of DNA have themselves interesting physical properties. Here we show that they can be used to prepare a DNA glass and we analyze the properties of this biological glass, in comparison with a glassy polymeric state.

The structure of the film strongly depends on that of DNA itself. The forces that hold the double helix together and stabilize the whole DNA structure are the hydrogen bonding and the stacking interactions between the bases. The weak interaction of the hydrogen bonds and, at the same time, the strong interaction between the sugar−phosphate backbone, allow large thermal fluctuations of the molecular structure at biological temperatures. These consist in local openings and closings of units of the base pairs. These sporadic dislocations of the helix are important for biology. For instance reading the genetic code requires the exposure of the bases to the surroundings after the opening of the pairs.

While the investigation of base-pair openings in the biological context is difficult, one can study these localized events as a pure physical process induced by heat. An increase of the temperature of the system induces cooperative openings of segments of base pairs, leading to the total disruption of the double helix at high temperature. This thermal denaturation of DNA is a transition from the ordered double helix to a random coil single stranded form. It is often called the "melting" of DNA.

To date, the thermal stability of DNA upon heating has been mostly investigated in solution, using techniques such as Raman spectroscopy, UV absorbance, and calorimetry.[4,5] We have used calorimetry and neutron scattering techniques to study the melting properties of DNA[2,3] in the form of films of oriented fibers made by the wet spinning technique.[6] A DNA fiber contains regions with crystalline order and others which are less organized.[7,8] It also includes hydration water which affects the structure of DNA.[9] In any case the proximity of the molecules within the fiber, although it does not preclude some conformational changes of DNA, results in a strong confinement which introduces local energy barrier for intermolecular motions.

The thermal denaturation of the DNA molecules has a strong effect on the whole structure of the fibers and films. In its double helix form DNA is fairly rigid, with a persistence length of about 500 Å. On the contrary the two single strands formed after denaturation are very flexible, with persistence lengths of the order of 10 Å. At high temperature this leads to a sample in which the strands are fully disordered and entangled, in a quasi-liquid state. In a rapid cooling to low temperature, lower than room temperature, the system undergoes a transition in which inter and intramolecular motions become too slow to be detectable experimentally. It is said to have gone through a glass transition. However, even though the stacking of the base pairs is broken, the intermolecular confinement is still present and influences the relaxation in the glassy state. The transition is observed within a temperature interval centered at a characteristic temperature, called the glass temperature T_g, at which the

Received: February 3, 2012
Revised: March 16, 2012
Published: March 20, 2012

ACS Publications © 2012 American Chemical Society

relaxation time of the system becomes of the order of the observation time. In the glassy region the nonequilibrium state slowly evolves toward equilibrium by structural relaxation (aging), but this relaxation becomes so slow that it can hardly be detected experimentally. If the temperature is lowered further the system appears as fully frozen. Its macroscopic properties, such as volume or enthalpy, become constant for the observer. The temperature at which one observes the glass transition is determined by the longest time scale accessible to the instrument.

Glasses are widely used materials, and the glass transition has been studied for decades, but its understanding is still an open problem.[10,11] The origin of the dramatic slowing down near T_g is probably strongly system dependent, and not yet fully understood. Microscopic approaches involve cooperatively rearranging regions in the Adam−Gibbs theory,[12] a continuously broken ergodicity that confines the system in a subspace of its phase space,[13] or more phenomenological approaches such as the mode coupling theory.[14] For polymers the entanglement of the molecular chains makes it very hard for the system to reach an equilibrium structure, and for single-stranded DNA relaxation may even be further hindered by the bases which are attached to the polymeric backbone.

Rather than attempting a microscopic description, one can try to apply the power of thermodynamics to glasses. Nonequilibrium thermodynamics introduces (at least) one additional variable ξ to measure the deviation from equilibrium. In combination with a model able to describe the relaxation time in a glass, this approach can be very fruitful to analyze thermodynamic measurements on a glassy system.[15,16] However the meaning of the ξ variable is not intuitive. Instead, to characterize the deviation from equilibrium, Tool[17] relied on the familiar concept of temperature, by introducing a "fictive temperature". Originally proposed as a convenient parameter in the manufacturing of glasses, this concept has led to many practical developments.[18] In the present paper we show how it can be applied to quantitatively characterize a DNA glass.

Earlier observations of glassy behavior of DNA have been done. At low temperature (∼240 K) slow relaxation can be assigned to the hydration water present in the samples.[19,20] Above room temperature, observations of the glassy behavior of DNA were done on hydrated powders[21] and fibers[22] but the calorimetric data were not quantitatively analyzed. In this paper, we report a detailed calorimetric study of the glassy behavior of films made from DNA fibers. We show that after the first irreversible thermal denaturation of the molecules upon heating, the sample reaches a disordered state in which it shows a typical glass behavior during successive cooling and heating scans. The fictive temperature is used to access the phenomenology of the DNA glass transition. For a further understanding we compare this glass transition aspect of melted DNA fibers with that of a classical polyvinyl acetate (PVAc) polymeric glass former.[23]

■ EXPERIMENTAL METHODS

Samples. *Preparation of DNA Films.* Deoxyribonucleic acid sodium salt from salmon testes was purchased from Sigma Co. Films were prepared by the "wet spinning apparatus technique".[6] The process consists in injecting a diluted solution of 1.58 g/L of DNA into a high concentrated EtOH solution (75% in 0.03 M NaCl). The DNA aggregates and consequently precipitates in the form of a very long thread, to finally be wound around a cylinder. This results in a film of adjacent oriented fibers of dimensions $8 \times 2 \times 5\ 10^{-3}$ cm^3. Gel electrophoresis shows that the length of the DNA molecules in the solution used to prepare the film and in a solution obtained by dissolving a piece of a fresh film is of the order of 20 kb or larger.[3]

After preparation a treatment of the film is necessary to control the DNA conformation, which could have been affected by the preparation process, particularly the presence of ethanol.[24] The samples were cleaned from salt excess for 24 h and dried for the same period of time using silica gel. For the purposes of our experiment, the samples were placed in desiccators with an oversaturated solution of NaBr in water, providing a relative humidity of 56%, for several weeks. The last step is crucial to determine the final structure of DNA. This hydration level insures a predominance of the A-form in the samples, although about 10% of B-form always remains.[9,25]

For each of the DSC experiments one piece of hydrated film, with a mass between 80 and 100 mg, was rolled up and placed in a Hastelloy tube having a volume of 1 mL. The open tube was then left inside the desiccator for a day to allow its content to reach the same relative humidity as the surroundings. Once this was accomplished, the tube was sealed with an O-ring to fix the water content throughout the experiment. The film inside the tube was in contact with the cylindrical wall, ensuring a good thermal contact. In most cases the space occupied by the film in the tube reached up to 3/4 of the total volume.

Getting a DNA Glass. The film was then subjected to an appropriate thermal treatment to obtain the DNA glass investigated in our studies. The Hastelloy tube containing the sample was inserted in the differential scanning calorimeter (DSC) at 293 K and left 10 min for stabilization. For the reference tube, 345 mg of polyimide trademark VESPEL was used. This polymer does not exhibit a glass transition within the region of our study, but establishes a linear baseline.

The sample was first cooled down to 268 K, where it was stabilized for 10 min. No signal associated to a freezing of the water was detected, which is not surprising as highly confined water or water in contact with biological molecules freezes well below 273 K.[26] This initial sequence was followed by DSC scans with increasing then decreasing temperatures. The increasing ramp was performed at 1.2 K/min, from 268 to 368 K. The sample was stabilized for one hour at this high temperature. Then we decreased temperature from 368 to 268 K at the rate of 1.2 K/min. The results are shown in Figure 1.

The heating curve shows two endothermic processes, one around 324 K and a more prominent one centered near 344 K. The first one is associated to a configurational change within the secondary structure of the DNA. It was previously discussed by Lee and co-workers as an endothermic process due to the loss of ordered structure driven by dehydration.[22] The large peak at 344 K corresponds to the thermal denaturation of DNA as seen in solution, a first order phase transition. This transition has been studied for decades on DNA solutions. Its observation with a DNA film shows that the confinement of the molecules in the fibers is not sufficient to prevent the separation of the two strands. As discussed in the Introduction, DNA thermal denaturation is accompanied by a sharp decrease of the persistence length of the molecules. This is associated to large fluctuations of the axis of the molecules, which are entropically favorable and lead to a partial loss of the orientational order that is also detected in neutron scattering experiments.

The cooling scan shows that, contrary to what is observed in solution for short DNA molecules, for the long molecules used

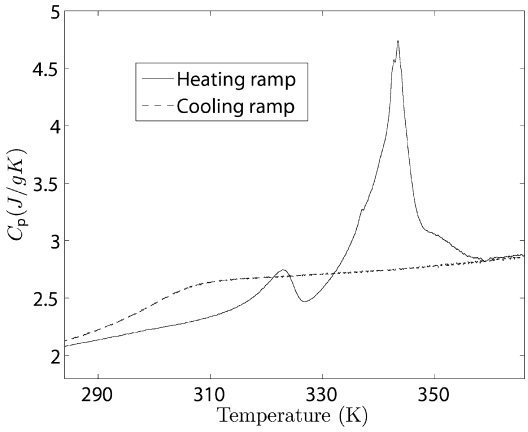

Figure 1. DSC heating scan of a film of oriented DNA fibers measured at 1.2 K/min (continuous line), followed by a cooling run at the same rate (discontinuous line).

in this experiment, and due to the confinement in the film, the denaturation of the double helix is not reversible. On cooling we do not find any exothermic peak corresponding to the large endothermic peak of the denaturation. Instead we observe a step-like descent in heat capacity, which is typical of a glass transition. Subsequent heating and cooling do not show the two endothermic peaks observed on the first heating, but instead features which are characteristic of a glass, and which are the object of this paper.

Before proceeding with each of the experiments to study the glass behavior of melted DNA, a protocol composed of a series of cooling−heating scans (pre-experiment) was performed to ensure a stabilization of the glass structure and to erase any previous thermal history. When starting a DSC experiment after placing the sample inside the DSC for the first time, or after finishing a DSC experiment, the sample is held isothermally at 293 K for at least 10 min. This is henceforth the initial temperature of the pre-experiment. The sample is then cooled to 268 K and left at that temperature for 10 min, heated to 363 K and held isothermally for 1 h. This is followed by cooling back to 268 K, maintaining this temperature for 10 min and heating thereafter to 363 K and stabilizing the sample at this temperature for 20 min. This state is the initial state for the different experimental procedures detailed below and summarized in Table 1. These cooling−heating runs were performed at a scanning rate of 1.2 K/min.

Preparing the PVAc Samples. PVAc is a polymeric glass former that is a reference in glass science. Its major advantage is that it does not crystallize during cooling, and its glass transition temperature is around room temperature. Consequently it has been extensively studied by various techniques and particularly by DSC, and useful data can be found in the literature.[23,27] However, care must be taken because it has a great tendency to absorb water, which influences its glassy properties.[28] For this study, we used samples made of small balls of about 100 mg, kindly given by Pr. G. McKenna. The average molecular weight is 157 kg/mol and the polydispersity index (PDI), which indicates the distribution of individual molecular masses in a polymer, is 2.73. The PVAc is first put in an oven under vacuum at a temperature of 105 °C, well above T_g, during 24 h in order to remove all the water from the melt. After a rapid mass measurement, the sample is put in the micro-DSC sealed Hastelloy tube for DSC measurements that follow exactly the same protocol as for the DNA sample.

DSC Experiments. A Setaram Micro-DSCIII has been used to perform the experiments. This is a highly sensitive heat flux-DSC with two 1-mL volume Hastelloy tubes for sample and reference. The tubes are enclosed in a highly conducting zone surrounded by thermopiles mounted in opposition. The temperature ramp is imposed by other thermopiles and a servo system using a circulating organic fluid allowing a very good temperature stability. The mass of the sample and reference-cells plus sensor (with or without sample and reference inside) is rather high, so that the maximum possible temperature rate (cooling or heating) is 1.2 K/min. This ensures that negligible temperature gradients exist even within liquid or polymeric samples. The high value of the calorimeter time constant ensures a good heat capacity resolution (or heat flux resolution) even for very low scanning temperature rates. In constant temperature mode the limit of detection is less than 1 μW. However, the large time constant has a perturbing influence on the heat capacity curves, particularly for glass transition study, as explained below, and the signal has to be properly deconvoluted to provide the instantaneous energy changes in the sample. The micro-DSCIII calorimeter is particularly adapted for low frequency fine thermal events probed with scanning temperature ramps in the range between 0.01 and 1.2 K/min. The water of the external stabilizating bath was held to 15 °C for all of the experiments.

Thermal Lag and Deconvolution of the Data from the Instrumental Response. As DSC scans involve a temperature variation, one must consider two effects in the analysis of the data. First a bad thermal contact between the sample or reference and the calorimeter probes, or the low value of the thermal diffusivity of some samples, could lead to spurious

Table 1. Table of Scanning Rates for the Different Experimental Procedures[a]

analysis thermal lag	different cooling rates	annealing at T_a at different t_a
363 K → 268 K → 363 K	363 K → 268 K → 363 K	363 K → T_a (for t_a^n) → 268 K → 293 K
$D_n \rightarrow M_n$ at q_n	$D_n \rightarrow M_n$ at q_n	t_a
$q_1(D_1/M_1) = 0.1/1.2$	$q_1(D_1/M_1) = 1.2/1.2$	$(t_a^1) = 84$, $(t_a^2) = 66$
$q_2(D_2/M_2) = 0.0833/1$	$q_2(D_2/M_2) = 0.4/1.2$	$(t_a^3) = 72$, $(t_a^4) = 66$
$q_3(D_3/M_3) = 0.066/0.8$	$q_3(D_3/M_3) = 0.2/1.2$	$(t_a^5) = 60$, $(t_a^6) = 54$
$q_4(D_4/M_4) = 0.416/0.5$	$q_4(D_4/M_4) = 0.1/1.2$	$(t_a^7) = 48$, $(t_a^8) = 42$
$q_5(D_5/M_5) = 0.033/0.4$	$q_5(D_5/M_5) = 0.05/1.2$	$(t_a^9) = 32$, $(t_a^{10}) = 20$
$q_6(D_6/M_6) = 0.025/0.3$	$q_6(D_6/M_6) = 0.033/1.2$	$(t_a^{11}) = 10$, $(t_a^{12}) = 6$
	$q_7(D_7/M_7) = 0.01/1.2$	$(t_a^{13}) = 3$, $(t_a^{14}) = 1$
	$q_8(D_8/M_8) = 1.2/1.2$	$(t_a^{15}) = 0$

[a]The temperatures are given in K; the scanning rate, q in K/min; and the annealing times, t_a in hours.

temperature gradients, and second the calorimeter has a finite response time that must be taken into account.

A preliminary experimental check was carried out to prove that the measurements did not account for any thermal lag. Indeed, general DSC instruments work with rather high scanning rate around 10 K/min or more. It induces the presence of temperature gradients inside the volume of the sample, or at the interfaces between the sample and the vessels. These unwanted gradients can deform the shape of the measured heat capacity curves and provide data with high inaccuracies. In the present case, the samples masses used were between 50 and 100 mg, and we have profited from the very low scanning temperature rates range of the calorimeter (between 10^{-3} and 1.2 K/min) to consider that such effects do not perturb our experiments. A second unwanted effect than can occur, is due to the presence of an external thermal time constant of the microcalorimeter. In the case of the glass transition study, neglecting this effect can completely suppress heat capacity overshoots during heating scans such as well described in ref 29 (see also the ref 30 where DSC thermal lag effects in glass studies have been discussed).

It has been theoretically proved that, in the absence of thermal lag, heating scans obtained from experiments in which the heating and cooling rates have a fixed ratio q_c/q_h result in peaks in specific heat which are exactly superposable by a shift along the temperature scale. Due to the thermal lag the usual experimental data are not superposable. Hodge[29] has recently given a procedure of deconvolution of the experimental data which is very effective to suppress the effects of the thermal lag. We use this procedure in our analysis. As a check and to probe the time constant effect, a protocol consisting of a series of cooling/heating cycles at different scanning rates but with constant cooling rate/heating rate (q_c/q_h = 0.833) ratio has been used. This consisted on temperature cycles of a first cooling ramp from 363 to 268K, 10 min of equilibration at that temperature, followed by a raise in temperature from 268 to 363 K, and again 20 min to allow the sample to stabilize. The cycles were repeated 7 times.

The data were deconvoluted from instrumental response using eq 1, where ΔP corresponds to the corrected heat flow, ΔP_0 is the measured heat flow, q the heating rate, and τ_0 corresponds to the calorimeter time constant. This characteristic constant can be extracted by monitoring the time it takes for the instrument to respond to an instantaneous power change, for example when turning off the DSC calibration heater. In our case, we have used the value of τ_0 = 60 s given by the supplier.

$$\Delta Cp_{\mathrm{DEC}} q = \Delta P = \Delta P_0(t) + \tau_0 \frac{\mathrm{d}\Delta P_0(t)}{\mathrm{d}t}$$

$$\Delta Cp_{\mathrm{DEC}} = \frac{\Delta P_0}{q} + \frac{\tau_0}{q}\frac{\mathrm{d}\Delta P_0}{\mathrm{d}t} \quad (1)$$

The deconvoluted data, Cp_{DEC}, corresponds to the difference in heat capacity of DNA and VESPEL cells; in order to isolate the DNA contributions, the VESPEL component has to be added to the total signal. The data are normalized by the sample mass, and finally presented in the form of Cp_{DNA} (J/gK). These can be summarized by the following mathematical expressions:

$$\Delta Cp_{\mathrm{DEC}} = m_{\mathrm{DNA}} Cp_{\mathrm{DNA}} - m_{\mathrm{VES}} Cp_{\mathrm{VES}}$$

$$Cp_{\mathrm{DNA}} = (\Delta Cp_{\mathrm{DEC}} + m_{\mathrm{VES}} Cp_{\mathrm{VES}})/m_{\mathrm{DNA}} \quad (2)$$

Figure 2 shows the heating curves for the same ratio of cooling rate to heating rate, comparing the deconvoluted data

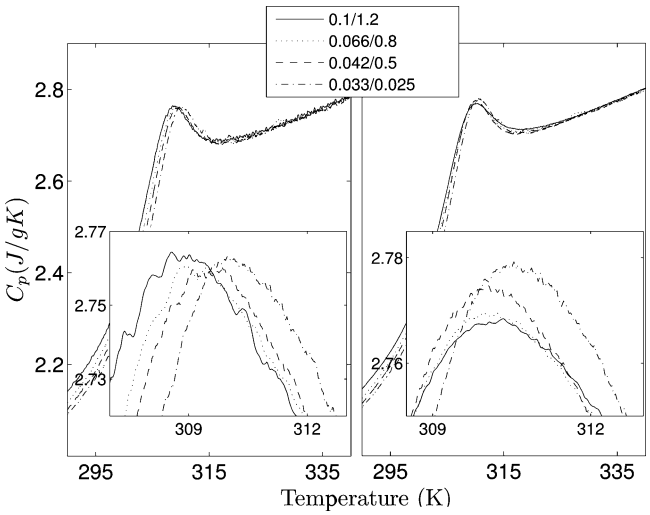

Figure 2. DSC heating scans at different heating rates, maintaining the ratio of cooling rate/heating rate constant. The image on the left shows the deconvoluted data for τ_0 = 60 s; the data on the second image has not been deconvoluted.

for τ_0 = 60 s (left), to that without deconvolution, τ_0 = 0 (right). The image of the left shows all peaks at the same amplitude.[29] This effect can only be attained when the data is deconvoluted with the right time constant, and no thermal lag due to a bad thermal contact of the sample within the pan occurs. With the comparison of both images we proved not only that the chosen calorimetric time constant is reliable, but also that the experiment was carried out with a uniform temperature within the cell and the sample (or reference).

Experimental Protocol. As discussed with the presentation of the protocol to get the DNA glass, each series of experiment is preceded by a "pre-experiment" to attempt to achieve a well-defined starting state of the sample. Two series of experiments were then carried out, with the same sample, to study the structural relaxation behavior of melted oriented DNA fibers via two methods.

Different Cooling Rates. This consisted in a succession of temperature ramps. Starting from the initial state at 363 K, the sample was cooled down at a rate q from 363 to 268 K, left for 5 min for equilibration, and heated up to 363 K at 1.2 K/min. It was then stabilized for 20 min at this highest temperature before the next cooling ramp, which was recorded as a DSC scan. The cooling rate was modified at each ramp in the following order, q = 1.2, 0.4, 0.2, 0.1, 0.05, 0.033, 0.01, and back to 1.2 K/min. The heating rate was kept fixed.

Annealing at Low Temperature for Different Aging Times. The procedure consisted in cooling at 1.2 K/min from 363 K to the aging temperature T_a below the glass transition temperature, annealing the sample for a period of time t_a, and then cooling down to 268 K before recording the DSC signal on heating from 268 to 363 K. All temperature ramps were programmed at a rate of 1.2 K/min. The relaxation of the system was studied at seven different aging times, t_a = 84, 78,

72, 66, 60, 54, 48, 42, 32, 20, 10, 6, 3, 1, and 0 h. The latter corresponds to an experiment without an actual annealing. However simply taking into account the minimal response time of the calorimeter one can consider that the effective minimal aging time is actually equal to 10 min.

DSC runs relevant to the paper have been summarized in Table 1.

RESULTS

Different Cooling Rates. Let us first consider the case of a series of experiments in which the sample is cooled at different rates q_n, as indicated in column 2 of Table 1 and then heated up at the rate of 1.2 K/min. Figure 3a shows the specific heat

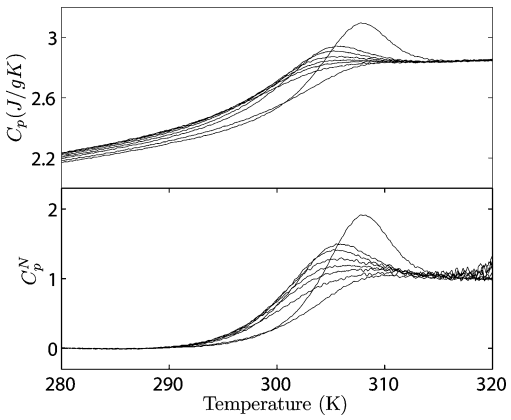

Figure 3. (a) DSC enthalpic response on heating at 1.2 K/min after cooling at different rates, q, the data is expressed in heat capacity versus temperature. (b) Normalized heat capacity (C_p^N) versus temperature. The numbers correspond to the index of the scan q_1 to q_8 in column 2 of 1.

$C_p(T)$ measured during each of the increasing temperature ramps. As expected for a typical glass,[18] it shows a fast rise in the glass transition temperature domain, and even a peak when the cooling has been sufficiently slow. This peak gets more and more pronounced as the cooling rate decreases. In the case of DNA one can notice that the highest peak (for the cooling rate q_7 = 0.01 K/min) appears shifted toward a higher temperature compared to the other measurements. After this measurement with a very low cooling rate, we again performed a scan with a cooling rate q_8 = 1.2 K/min, i.e. identical to the cooling rate q_1 of the first experiment. This last scan gives a curve $C_p(T)$ which is different from the curve recorded in the first scan, in the same conditions, indicating that, after the series of experiments involving a very slow cooling, the DNA sample has evolved.

To go beyond these qualitative observations, one needs a quantitative evaluation of the glassy relaxation in the system. The concept of "fictive temperature" was introduced precisely for this purpose.[17,18] The idea is that one can define a temperature $T_{f,p}$ such that a property p of a system in a glassy state at a low temperature T^* is the same as for a liquid equilibrated at the temperature $T_{f,p}$ and then quenched instantly to T^*, i.e.

$$p(T^*) = p(T_l) - \alpha_l(T_l - T_{f,p}) - \alpha_g(T_{f,p} - T^*) \tag{3}$$

where T_l is a temperature high enough for the system to be in the liquid state, and α_l and α_g designate the slope dp/dT in the liquid and glass states respectively. In the general case the state at temperature T^* can be any nonequilibrium state reached on cooling. When the temperature T^* is sufficiently low for the system to be in a glassy state where $(dp/dT)(T^*) = \alpha_g$, the fictive temperature is denoted by $T'_{f,p}$. All of the states of the same glass (i.e., reached by a given cooling rate) at different temperatures below the glass transition region have the same $T'_{f,p}$, which is a feature of the thermal history of the sample.

Obviously this concept, which describes the glassy state with a single parameter has some limitations.[31] Among others the fictive temperature $T_{f,p}$ depends on the particular property p which is considered. However this is a very useful phenomenological quantity because its analysis can be used to characterize the glassy state. In the context of calorimetry measurements, the quantity of interest is the specific enthalpy, and its derivative α is the specific heat C_l, for the liquid state, or C_g for the glassy state. It follows from eq 3 that the corresponding fictive temperature, denoted henceforth by T_f, can be obtained from the relation

$$\int_{T^*}^{T_l} [C(T') - C_g(T')]\, dT' = \int_{T_f}^{T_l} [C_l(T') - C_g(T')]\, dT' \tag{4}$$

It is also useful to introduce the normalized specific heat

$$C_p^N(T) = \frac{C(T) - C_g(T)}{C_l(T) - C_g(T)} \tag{5}$$

which is plotted in Figure 3b. To determine T_f with eq 4 and to calculate $C_p^N(T)$ one has to use the value of C_g which is observed for the particular glass (i.e., the particular cooling rate) of interest.

To analyze our results we have chosen a temperature T^* = 279 K which is sufficiently low to correspond to the glassy state. The values that we calculate are therefore the values of T'_f. They depend on the cooling rate q used to reach T^*. For the calculation with eq 4, the liquid and glass specific heats $C_l(T)$ and $C_g(T)$ are obtained by extrapolation from the low or high temperature specific heats respectively.

Figure 4 shows the fictive temperature, T'_f, as a function of cooling rate for a denatured sample of DNA. As expected T'_f decreases when the cooling rate decreases. Cooling more slowly let the system evolve longer at each temperature, i.e., extends the range for the relaxation times which are accessible for the system: the observable relaxation time τ evolves as the inverse of the cooling rate q, $\tau \propto 1/q$. Therefore lower cooling rates allow the system to move further along the equilibrium liquid state curve, i.e., to a lower fictive temperatures than fast cooling.

The concept of fictive temperature amounts to assuming that it would be equivalent for the system to follow the equilibrium curve down to the temperature T'_f and then be instantaneously frozen in a glassy state. We can therefore assume that the relaxation time in the glass is governed by an equilibrium-type Arrhenius law with respect to the temperature T'_f instead of the actual temperature. The fairly small range of time scales accessible in a calorimetry experiment, compared for instance to dielectric measurements that can observe much faster events, makes it less likely for calorimetry to detect deviations from the Arrhenius behavior. This is expressed as

$$\tau \propto \frac{1}{q} \propto \exp\left(\frac{\Delta h}{T'_f}\right) \tag{6}$$

where Δh is the typical energy barrier governing the relaxation.

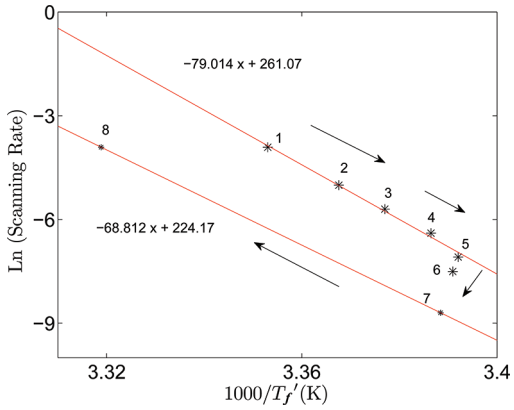

Figure 4. Dependence of T'_f on the cooling rate q. The symbols represent the values T'_f calculated with eq 4 for each experiment, while the solid line corresponds to a linear fit. The top fit includes the five points lying on it, which corresponds to the fastest cooling rates q = 1.2, 0.4, 0.2, 0.1, and 0.05 K/min). The point corresponding to q_6 = 0.033 K/min was excluded. The fit below was obtained with the last cooling scans, q_7 = 0.01 and q_8 = 1.2 K/min arising at a higher T'_f. The equations for each of the fits are also shown on the plot. The arrows indicate the time-evolution of the system, also marked by numbers. Between the first measurement (number 1) and the last one (number 8), there was a period of ten days, corresponding to the cumulative time of the experiments.

Figure 4 shows that, for q = 1.2 K/min down to q = 0.05 K/min, eq 6 is well verified as $\ln(q)$ versus $1000/T'_f$ is a straight line. Its slope corresponds to Δh_{DNA} = 79 kK, i.e., a value comparable to the values which are obtained from a similar analysis in polymer samples such as PVAc which leads to Δh_{PVAc} = 99 kK.

However, for the slowest cooling rates q_6 = 0.033 and q_7 = 0.01 K/min, the experimental points show a systematic deviation from the Arrhenius curve, suggesting some evolution of the sample, facilitated by a process in which the system has been staying a very long time at high and moderate temperatures. A new measurement with q_8 = 1.2 K/mn after the sample has passed through this step of extremely slow cooling leads to a point on Figure 4 which does not coincide with the first point, obtained with the same cooling rate q_1 = 1.2 K/min. This attests of an irreversible evolution in the DNA sample. The slope of the line connecting the last two points q_7 = 0.01 K/min and q_8 = 1.2 K/min corresponds to Δh = 68.8 kK, a bit lower than the value found before this evolution of the sample.

Before attempting any discussion of these results which depart from the observations on a polymer like PVAc for which the Arrhenius plot is valid for all of the cooling rates, let us examine the second series of experiments, involving aging at constant temperature.

Annealing with Different Aging Times. As discussed when we introduced the experimental protocols, a second series of experiments was carried out to investigate the time evolution of the sample submitted to aging in the glassy state. This study was compared with a similar set of measurements for PVAc. The samples were annealed at a temperature T_a which is 15 K below the inflection point of their respective specific heat curve measured during the cooling run at 1.2 K/min, i.e., $T_{a,DNA}$ = 293 K and $T_{a,PVAc}$ = 297 K for DNA and PVAc. We investigated a series of aging times (relaxing times) t_a varying from 84 h to 1 h, and even no aging at all, as indicated in Table 1. The aging temperatures $T_{a,DNA}$ and $T_{a,PVAc}$ had been chosen to be low enough to ensure that the samples were in the nonequilibrium state. By selecting the same temperature drop of 15 K below the glass transition temperature of each sample, we expected the relaxation times to be comparable for the DNA and PVAc annealing studies. Our results show that this was not the case.

Figure 5 shows the DSC scans obtained by heating two samples at 1.2 K/min above the annealing temperature:

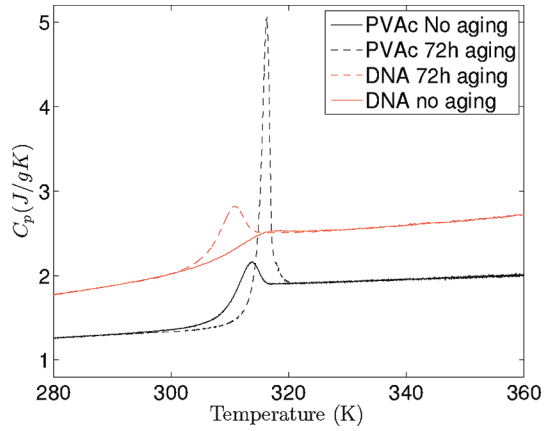

Figure 5. Comparison of the effects between nonannealed and annealing for 72 h of two different samples, denatured DNA and PVAc. For each sample the plotted curves are DSC scans recorded upon heating at 1.2 K/min.

denatured DNA (red) and PVAc (black). Nonannealed (continuous line) and 72 h annealed (dash line) scans were chosen to compare the glassy behavior of these samples upon aging. From the curves we can conclude that both samples behave in a qualitatively similar way: the annealed scans show a prominent peak at a temperature T_p higher than the annealing temperature T_a. However for PVAc a peak is visible during reheating even without aging, while for DNA there is no peak in the absence of aging. This suggests that underlying relaxation mechanisms for the two glass-formers do not obey the same laws. The comparison of the two peaks in the increasing temperature ramps after the same period of aging is more difficult because the aging temperatures are different. This is the object of the experiments described below.

Following the annealing, as discussed in the protocol section, the samples are cooled down to 268 K at the rate of 1.2 K/min, stabilized for 10 min at this temperature and then the measurement scan is identical to the ones that we performed for the various cooling rates; that is, we record the DSC signal while heating from 268 to 363 K. Therefore the measurement actually characterizes a system which has been frozen in its glassy state after aging. Figure 6a shows DSC heating scans for melted DNA annealed with different annealing times t_a. The progressive growth of an endothermic peak as t_a increases is clearly visible. Figure 6b shows the difference curves of the annealed scans with respect to the nonannealed, t_a = 0, used as reference curve. The effects of the increase of the peak as well as the change in the peak position appear more clearly in this plot.

The state of the sample after annealing can be characterized by two quantities. First the area between the annealed and unannealed scans, often called "enthalpy recovery" ΔH corresponds to an enthalpy decrease during the annealing process, which is again absorbed by the system to reach the

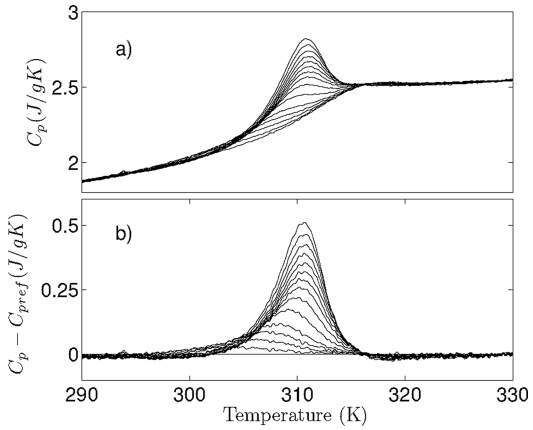

Figure 6. (a) Heat capacity versus temperature of denatured DNA annealed at 293 K for different t_a (in hours) = 84, 78, 72, 66, 60, 54, 48, 42, 32, 20, 10, 6, 3, 1, and 0; the latter corresponds to that of nonannealed. (b) Heat capacity versus temperature for the corresponding DSC difference curves, C_p(annealed)−C_p(unannealed), for each aging time t_a.

equilibrium state at high temperature. It characterizes the annealed glassy state from the energetic viewpoint. Second the notion of fictive temperature, that we used in the previous section to characterize glassy states obtained at different cooling rates, is also pertinent to describe the internal state of the glass in the context of aging. Owing to our experimental protocol, in which we freeze the system to low temperature (268 K) before recording the DSC signal with increasing temperature, when we apply eq 4 to the specific heat curves of Figure 6, we obtain a value of T'_f, which characterizes the frozen state obtained after aging.

As expected the enthalpy recovery increases with the aging time, while the effective temperature decreases (Figure 7). The

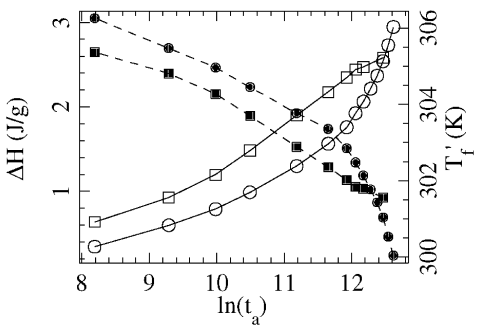

Figure 7. Aging of the DNA and PVAc samples. The circles refer to DNA results and the squares to PVAc. Open symbols and full lines: enthalpy recovery ΔH as a function of the logarithm of the aging time (in seconds). Filled symbols and dash lines: fictive temperature T'_f as a function of the logarithm of the aging time (in seconds).

curves for DNA and PVAc show however a difference. For PVAc, for the longest aging times, one can notice the beginning of a saturation, as the variation of ΔH and T'_f appears to slow down. This suggests that the longer waiting time used in our experiment, 84 h, approaches the relaxation time of the PVAc glass for $T = T'_f = T_a$. This is not the case for DNA. Even for the longest aging times the evolution of the glass continues, without a sign of a saturation.

As we have two quantities to characterize aging, it is interesting to check whether they actually detect the same underlying phenomena during aging. For this purpose we can rescale the data by calculating the reduced quantities

$$\Delta H_{red} = \frac{\Delta H(t_a) - \Delta H_{min}}{\Delta H_{max} - \Delta H_{min}} \tag{7}$$

where ΔH_{max} and ΔH_{min} are respectively the maximum value of ΔH (for the longest aging time) and the minimum value of ΔH (for the shortest aging time), and similarly

$$T'_{f,red} = \frac{T'_{f,max} - T'_f(t_a)}{T'_{f,max} - T'_{f,min}} \tag{8}$$

where $T'_{f,max}$ and $T'_{f,min}$ are the maximum and minimum values of T'_f (for the shortest and longest waiting times).

Figure 8 shows that these two quantities evolve very similarly when the aging time grows. For the smallest aging times of

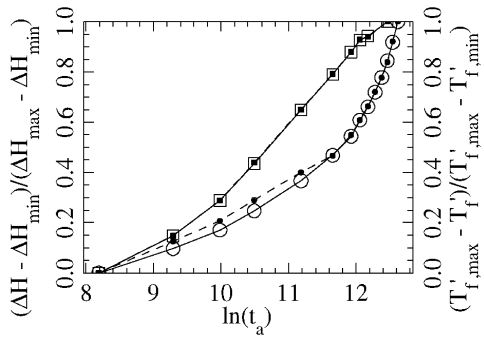

Figure 8. Aging of the DNA and PVAc samples. The circles refer to DNA results and the squares to PVAc. The figure shows with open symbols the reduced enthalpy recovery ΔH_{red} defined by eq 7 as a function of the logarithm of the aging time (in seconds). The filled symbols show the reduced fictive temperature $T'_{f,red}$ defined by eq 8, as a function of the logarithm of the aging time (in seconds).

DNA one can observe a slight difference between the two curves, but it is within the experimental errors. The data are less accurate for DNA than for PVAc because, for DNA, at the smallest waiting times, the evolution of the system is small (as shown for instance on Figure 6b), and a slight error in the determination of the baseline leads to a significant relative error in ΔH. For PVAc the two evolutions are identical.

Actually this result could have been expected if one considers the meaning of the fictive temperature as it is sketched on Figure 9. For any state of the system, its fictive temperature is defined on a diagram showing enthalpy H versus temperature T by the intersection of a line with a slope equal to the glass specific heat C_g and the line describing the equilibrium state with slope C_l, i.e., the slope of the H versus T curve in the high temperature range. As a result, for point A on the diagram, the quantity ΔH_{red} is measured by the ratio of the length of the two segments A_1A/A_1A_2. Similarly the quantity $T_{f,red}$ is given by the ratio B_1B/B_1B_2. Simple geometry considerations show that these two ratios are equal.

However the equality would no longer be valid if the equilibrium curve for $H(T)$ were highly nonlinear in the range of the fictive temperatures involved, or if a unique fictive temperature was not sufficient to describe the state of the glass. Our experimental observation therefore suggests that the fictive temperature does provide a good description of the PVAc and DNA glasses.

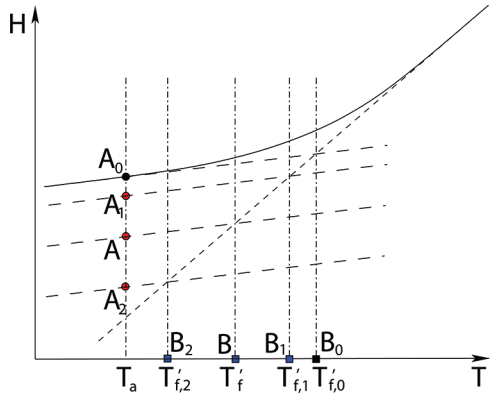

Figure 9. Evolution of the enthalpy and fictive temperature during aging. The starting point of the aging experiments is A_0. During the shortest aging time the system evolves from A_0 to A_1. Its enthalpy change is measured by the segment A_0A_1 and its fictive temperature evolves from $T'_{f,0}$ to $T'_{f,1}$. For an intermediate time the system evolves from A_0 to A and for the longest aging time it evolves from A_0 to A_2.

To get another view of the aging process, one can try to determine how the relaxation time evolves during the aging process. It seems reasonable to assume that, at the beginning of its aging, a system evolves faster because it explores the "easy paths" for relaxing. Then, once those paths are exhausted, the relaxation becomes harder. We cannot measure this directly, but, as we determine the fictive temperature $T'_f(t_a)$ as a function of the aging time, and if we assume the validity of eq 6 that we have tested in the experiments with different cooling rates, we obtain

$$\tau(t_a)/\tau(t_a = 0) = \exp\left[\Delta h\left(\frac{1}{T'_f(t_a)} - \frac{1}{T'_f(t_a = 0)}\right)\right] \tag{9}$$

Figure 10 shows this calculated evolution of the ratio $\tau(t_a)/\tau(t_a = 0)$ as the aging proceeds for DNA and for PVAc. The

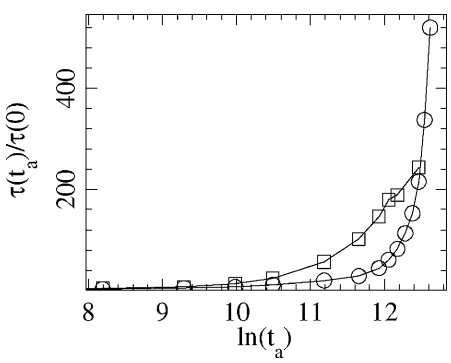

Figure 10. Evolution of the relaxation time versus aging. This figure shows the ratio of the relaxation time after an aging during t_a to the relaxation time without aging $\tau(t_a)/\tau(t_a = 0)$, assuming that the relaxation time follows the Arrhenius law eq 6. The circles correspond to DNA and the squares to PVAc.

relaxation time grows faster for PVAc than for DNA in the initial stage of aging, but then for long aging periods, while the relaxation time for PVAc tends to stabilize, the value of τ for DNA increases drastically. In terms of a free energy landscape, it would mean that, for DNA, after an initial period during which the glass can rearrange, the system falls into deep metastable minima from which it is very hard to exit. This can be related to the decrease of the enthalpy recovery for DNA for the longest aging times.

■ DISCUSSION

Our calorimetric study of a DNA film has shown that, after the thermal denaturation of the double helix, this system has properties which are very similar to those of a polymer glass, such as PVAc, with however noticeable differences

- an irreversible evolution of the DNA sample is observed when it is cooled extremely slowly.
- when it is annealed at low temperature, the DNA sample shows a very long relaxation time. Even after 84 h of annealing, 15 K below the glass transition temperature, the DNA sample still evolves significantly while PVAc starts to show some saturation.

These two effects are probably linked and related to the particular structure of DNA. The denatured strand of DNA is made of a sugar−phosphate backbone that carries large side groups, the A, T, G, and C bases which have the shape of flat single or double organic rings. The presence of these bases may affect the relaxation of the DNA glass in several respects: (i) by making the reptation of the polymer more difficult and (ii) because the bases tend to stack on top of each other, or may form hydrogen bonds with complementary bases.

Our experiments show that the enthalpy barrier Δh associated to the relaxation in the DNA film is of the same order of magnitude (80 kK) as the enthalpy barrier measured for PVAc (100 kK). This suggests that the slow relaxation in DNA come from kinetic factors, due to the confinement effect in the fibers. In the slow cooling experiments the system stays a long time at high temperature, which allows a faster exploration of the phase space. This could explain why its irreversible evolution is only observed in this case. The microscopic origin of this evolution is difficult to assert, but it could be associated to a partial stacking of the bases in some regions of the sample. In double stranded DNA the stacking interaction is known to contribute significantly to the stabilization of the double helix structure. Moreover, even in solution, the bases tend to stack, so that a partial stacking is plausible within the fibers too. But, as it requires large amplitude motions of big organic groups in a very confined environment, it is certainly a very slow process unless it can be assisted by thermal fluctuations. Moreover, a slow stacking of the bases, occurring in the last stage of a long relaxation of the DNA sample would be associated to an enthalpy gain. This would be consistent with our observation that the enthalpy recovery for the DNA sample exceeds that of PVAc (Figure 7) for the longest aging times.

However we cannot rule out other phenomena to explain the irreversible evolution of the DNA samples, in particular the role of the hydration water. It could be expelled from the bulk of the film during the slow cooling and accumulate in the part of the sample holder which is not fully filled by the DNA film.

This investigation has shown that the fiber form of DNA, prepared in the form of a film, has interesting physical properties which pose some questions for their understanding. DSC calorimetry is a useful tool to investigate the physical properties of this system, provided it is completed by some quantitative analysis. Using the fictive temperature allows further explorations of the relaxation processes, in particular because it gives an estimate of their enthalpy barrier. For a complete microscopic understanding this method has never-

theless to be completed by other approaches, such as structural studies with neutron scattering[3] or perhaps spectroscopic investigations.

■ AUTHOR INFORMATION

Corresponding Author

*E-mail: valleorero@ill.fr; Michel.Peyrard@ens-lyon.fr.

Notes

The authors declare no competing financial interest.

■ REFERENCES

(1) Watson, J.; Crick, F. *Nature* **1953**, *171*, 737−738.
(2) Wildes, A; Theodorakopoulos, N.; Valle-Orero, J.; Cuesta-López, S.; Garden, J.-L.; Peyrard, M. *Phys. Rev. Lett.* **2011**, *106*, 048101.
(3) Wildes, A; Theodorakopoulos, N.; Valle-Orero, J.; Cuesta-López, S.; Garden, J.-L.; Peyrard, M. *Phys. Rev. E* **2011**, *83*, 061923.
(4) Duguid, J.; Bloomfield, V.; Benevides, J.; Thomas, G. *Biophys. J.* **1996**, *71*, 3350−3360.
(5) Wartell, R. M.; Benight, A. S. *Phys. Rep.* **1985**, *126*, 67−107.
(6) Rupprecht, A. *Biochem. Biophys. Res. Commun.* **1963**, *12*, 163−168.
(7) Langridge, R.; Wilson, H. R.; Hooper, C. W.; Wilkins, M. H. F.; Hamilton, L. D. *J. Mol. Biol.* **1960**, *2*, 19−37.
(8) Langridge, R.; Marvin, D. A.; seed, W. E.; Wilson, H. R.; Hooper, C. W.; Wilkins, M. H. F.; Hamilton, L. D. *J. Mol. Biol.* **1960**, *2*, 38−64.
(9) Fuller, W.; Forsyth, T.; Mahendrasingam, A. *Phil. Trans. R. Soc. London B* **2004**, *359*, 1237−1248.
(10) Berthier, L.; Biroli, G. *Rev. Mod. Phys.* **2011**, *83*, 587−645.
(11) Debenedetti, P. G.; Stillinger, F. H. *Nature* **2001**, *410*, 259−267.
(12) Adam, G.; Gibbs, J. H. *J. Chem. Phys.* **1965**, *43*, 139−146.
(13) Mauro, J. C.; Gupta, P. K.; Loucks, R. J. *J. Chem. Phys.* **2007**, *126*, 184511−1−11.
(14) Kirkpatrick, T. R. *Phys. Rev. A* **1985**, *31*, 939−944.
(15) Möller, J.; Gutzow, I.; Schmeltzer, J. W. P. *J. Chem. Phys.* **2006**, *125*, 094505−1−13.
(16) Garden, J.-L.; Guillou, H.; Richard, J.; Wondraczek, L. *J. Non-Equilib. Thermodyn.* **2012**, DOI: 10.1515/jnetdy-2011-0036[dx.doi.org].
(17) Tool, A. Q. *J. Am. Chem. Soc.* **1931**, *14*, 276−308.
(18) Hodge, I. M. *J. Non Cryst. Solids* **1994**, *169*, 211−266.
(19) Rüdisser, S.; Hallbrucker, A.; Mayer, E. *J. Phys. Chem.* **1996**, *100*, 458−461.
(20) Rüdisser, S.; Hallbrucker, A.; Mayer, E.; Johari, G. P. *J. Phys. Chem. B* **1997**, *101*, 266−277.
(21) Tsetereli, G. I.; Belopolskaya, T. V.; Gruinina, N. A.; Vaveliouk, O. L. *J. Thermal Anal. Calorim.* **2000**, *62*, 89−99.
(22) Lee, S. L.; Debenedetti, P. G.; Errington, J. R.; Pethica, B. A.; Moore, D. J. *J. Phys. Chem. B* **2004**, *108*, 3098−3106.
(23) Svoboda, R.; Honcova, P.; Malek, J. *Polymer* **2008**, *49*, 3176−3185.
(24) Piškur, J.; Rupprecht, A. *FEBS Lett.* **1985**, *375*, 174−178.
(25) Krisch, M.; Mermet, A.; Grimm, H.; Forsyth, V.; Rupprecht, A. *Phys. Rev. E* **2006**, *73*, 061909−1−10.
(26) Spanoudaki, A.; Albela, B.; Bonneviot, L.; Peyrard, M. *Eur. Phys. J. E* **2005**, *17*, 21−27.
(27) Hutchinson, J. M.; Kumar, P. *Thermochim. Acta* **2002**, *391*, 197−217.
(28) Beiner, M.; Korus, J.; Lockwenz, H.; Schröter, K.; Donth, E. *Macromolecules* **1996**, *29*, 5183−5189.
(29) Hodge, I. *J. Non-Cryst. Solids* **2010**, *356*, 1479−1487.
(30) Hutchinson, J. M.; Ruddy, M.; Wilson, M. R. *Polymer* **1988**, *29*, 152−159.
(31) Ritland, H. *J. Am. Ceram. Soc.* **1956**, *39*, 403−406.